Journal of
Composites Science

MDPI

Article

A Novel One-Pot Synthesis of PVP-Coated Iron Oxide Nanoparticles as Biocompatible Contrast Agents for Enhanced T_2-Weighted MRI

Fedda Y. Alzoubi [1], Osama Abu Noqta [1,2,*], Tariq Al Zoubi [3,*], Hasan M. Al-Khateeb [1], Mohammed K. Alqadi [1], Abdulsalam Abuelsamen [4] and Ghaseb Naser Makhadmeh [1,*]

[1] Physics Department, Jordan University of Science and Technology, Irbid 22110, Jordan
[2] Nano-Biotechnology Research and Innovation (NanoBRI), Institute for Research in Molecular Medicine (INFORMM), Universiti Sains Malaysia, Pulau Pinang 11800, Malaysia
[3] College of Engineering and Technology, American University of the Middle East, Egaila 54200, Kuwait
[4] Medical Imaging and Radiography Department, Aqaba University of Technology, Aqaba 910122, Jordan
* Correspondence: osama1987ahmad@yahoo.com (O.A.N.); tariq.alzoubi@aum.edu.kw (T.A.Z.); ghaseb84@yahoo.com (G.N.M.)

Abstract: A contrast agent with specific characteristics is essential for high-quality magnetic resonance imaging (MRI). It plays a crucial role in enhancing the visibility of certain tissues and structures, making it imperative for diagnostic procedures. Superparamagnetic iron oxide nanoparticles (SPIONs) have emerged as a promising alternative to traditional contrast agents for MRI due to their non-toxicity and superior magnetic properties. However, a suitable surface coating strategy is needed to produce polymer-coated SPIONs with controllable sizes in order to enhance their stability and biocompatibility. This study presents a novel one-pot synthesis method for the production of highly stable polyvinylpyrrolidone (PVP)-coated SPIONs. By systematically manipulating the physicochemical properties of SPIONs, the effect of different molecular weights of PVP was studied. The results showed that SPIONs coated with PVP with molecular wight 40,000 g/mol (40 K) exhibited a high magnetization (Ms = 48.4 emu/g), an average size distribution (11.61 nm), and excellent stability. The relaxivity of coated and uncoated SPIONs was investigated using MRI images. The results revealed that the (r_2/r_1) ratio of PVP40K-SPIONs was 72.55, compared to 55.72 for the bare SPIONs, making them a highly promising T_2-contrast agent for future development of MRI applications. This study opens new avenues for the development of biocompatible and stable SPIONs for improved medical diagnostic and imaging.

Keywords: PVP; superparamagnetism; iron oxide nanoparticles; polyvinylpyrrolidone; molecular weight; MRI

Citation: Alzoubi, F.Y.; Abu Noqta, O.; Al Zoubi, T.; Al-Khateeb, H.M.; Alqadi, M.K.; Abuelsamen, A.; Makhadmeh, G.N. A Novel One-Pot Synthesis of PVP-Coated Iron Oxide Nanoparticles as Biocompatible Contrast Agents for Enhanced T_2-Weighted MRI. *J. Compos. Sci.* **2023**, *7*, 131. https://doi.org/10.3390/jcs7030131

Academic Editor: Francesco Tornabene

Received: 6 February 2023
Revised: 10 March 2023
Accepted: 17 March 2023
Published: 22 March 2023

1. Introduction

Contrast-enhanced magnetic resonance imaging (MRI) is a widely recognized and highly effective non-invasive clinical technique for the evaluation of anatomy and tissue function. MRI contrast agents are substances injected into the body to enhance the visibility of internal structures and differentiate between normal and abnormal tissues. These agents serve to improve the visibility of certain body tissues, organs, and structures, resulting in a more accurate diagnosis and an improved treatment plan. The selection of the appropriate contrast agent is imperative to the continued development of MRI technology. The commonly used contrast agents in MRI, such as Gd-DTPA, exhibit rapid clearance via renal excretion, as well as a short residence time within organs, such as the liver [1,2]. Furthermore, there have been recent concerns raised regarding the potential harmful effects of Gd-DTPA on kidney functions. In light of these limitations, there is a significant need to identify and develop biocompatible MRI contrast agents with prolonged

imaging time-windows and gradual excretion mechanisms. To address these challenges, MRI images can be further improved by the incorporation of contrast agents that alter the transverse relaxation time (T_2), making it an even more valuable diagnostic tool. In this context, superparamagnetic iron oxide nanoparticles (SPIONs) have attracted significant attention from researchers for their exceptional characteristics, such as high relaxivity, superior magnetic properties, non-toxicity, and the ability to target specific cells or tissues. Compared to Gd-based contrast agents, SPIONs have proved to be promising nanomaterials for a wide range of biomedical applications [3–6].

SPIONs nanoparticles can be functionalized with various molecules, making them useful in applications, such as hyperthermia, catalysis, drug delivery, and as interesting alternative contrast agent in magnetic resonance imaging (MRI) [7]. In MRI applications, SPIONs should have a suitable particle size, chemical stability under physiological conditions, and specific magnetic characteristics [8]. To overcome this limitation, SPIONs need to be stabilized with biocompatible materials on their surface, such as chatoyant, citric acid, starch, and polyvinylpyrrolidone (PVP) [9]. Polyvinylpyrrolidone (PVP) is an amphiphilic, non-toxic, and biocompatible polymer that comprises C=O, C-N, and CH_2 functional groups [10]. These functional groups make PVP an ideal choice for stabilizing and functionalizing SPIONs. Furthermore, PVP can increase the stability of SPIONs by reducing particle aggregation and improving their dispersibility in biological fluids. As a result, the different functional groups of the PVP molecule interact differently with SPION surfaces. For example, C=O and C-N groups form strong bonds with the SPIONs, while the CH_2 groups provide stability and flexibility by allowing the PVP molecules to move around the surface. In this way, the PVP molecules can protect the SPIONs from aggregation and help to keep them stable [11,12]. Therefore, the PVP molecule plays important roles in the stabilizing of SPIONs, as well as in providing a biocompatibility shell. This can be attributed to the fact that the polar head groups of PVP can be absorbed into the surface of SPIONs, whereas the chain groups can adjust the distance between the adsorbed head groups [13,14]. Previous studies have focused only on the effect of PVP concentration on the size of SPIONs. For instance, Zhang et al. investigated the effect of PVP concentration on the synthesis of ultra-small SPIONs via the coprecipitation method at 75 °C [15,16]. Lee et al. studied the effect of the molar ratio of PVP/Fe $(CO)_5$ on the particle size of magnetic nanoparticles using the one-step method [17]. Yet, regardless of the achievements mentioned above, there has been almost no report on the influence of PVP molecular weight on the SPIONs' size and stability. There is, however, a lack of research on the effect of PVP molecular weight on the size and stability of these nanoparticles.

This study aims to bridge this gap by investigating the effect of PVP molecular weight on the particle size and stability of SPIONs as a contrast agent for T_2-weighted magnetic resonance imaging (MRI). A better understanding of the relationship between PVP molecular weight and SPIONs will enable us to optimize their performance as MRI contrast agents. Moreover, this study will reveal an effective coating strategy for adding iron precursors and PVP solution to the reactor, thereby improving the efficiency of SPION synthesis. The outcomes of this study hold great potential for improving the use of SPIONs in MRI technology by developing stable and efficient nanoparticles. As a result, a thorough understanding of PVP-coated SPIONs and their physical properties could provide insights into the intricate mechanisms of MRI imaging, thus enabling the development of more effective nanoparticles for MRI applications. This would lead to more accurate diagnostic results for patients, which in turn could lead to more targeted and effective treatment plans, as well as better outcomes for patients.

2. Materials and Methods

2.1. Materials

All chemical materials utilized in this study were procured from Sigma Aldrich (14508 Saint Louis, MO 63178, United States), including iron (III) chloride hexahydrate ($FeCl_3 \cdot 6H_2O$, >99% purity), iron (II) chloride tetrahydrate ($FeCl_2 \cdot 4H_2O$ > 99% purity), sodium hydroxide (NaOH > 98% purity), and polyvinylpyrrolidone (PVP) with average

molecular weights of 10,000, 25,000, and 40,000. These materials were employed as received, without any further purification, in order to ensure consistency and reproducibility of experimental results. To guarantee the highest level of purity and quality, Milli-Q water with resistivity of 18.2 $M\Omega.cm^{-1}$ was utilized throughout the synthesis and preparation of magnetic nanoparticles.

2.2. One-Pot Synthesis of PVP-Coated SPIONs Nanoparticles

A novel one-pot method was used to synthesize PVP-coated superparamagnetic iron oxide nanoparticles (PVP-SPIONs). The one-pot method combined all the necessary components in a single reactor vessel while simultaneously adding a surfactant and a base. This helps to ensure that the molecules form the desired nanoparticles with a narrow size distribution and high homogeneity. The different molecular weights of PVP also help to control the rate of reaction and the size of the nanoparticles formed. Following is a brief description of the procedure. A total of 0.5 g of polyvinylpyrrolidone (PVP) with different molecular weights (MWs) were dispersed in distilled water for 15 min at 80 °C with different stirring speeds. The PVP was dissolved in distilled water in order to create a homogenous solution.

A mixture of 2.0 millimoles of Fe^{2+} and 1.0 millimoles of Fe^{3+} was dissolved in 25 milliliters of distilled water at room temperature in two glass beakers. The Fe^{2+} and Fe^{3+} were dissolved in a separate solution in order to create a mixture, which was then added to the PVP solution. The beakers were then carefully mixed, and the reaction was allowed to proceed for 1 h, after which the reaction was stopped by cooling the beakers to room temperature. The reactant solutions were then added to the reactor under nitrogen protection and a stirring speed of 600 rpm using peristaltic pumps at a flow rate of 0.1 L/min, as shown in Figure 1. The pH value of the reaction was controlled at 10 using 1.0 M NaOH solution through titration with a 842 Titrando Metrohm pH meter (Metrohm, Herisau, Switzerland). After 1 h of stirring, the solution was cooled to room temperature by removing the heat source. The black precipitate was collected with a strong magnet and washed several times with distilled water. As a result of completing the fabrication process, PVP-coated SPIONs were dried to obtain samples A, B, C, and D. Sample A is bare-SPION synthesized at 80 °C with 0.5 g PVP, Sample B is PVP-10k-SPION synthesized at 80 °C with 0.5 g PVP-10000, Sample C is PVP-25k-SPION synthesized at 80 °C with 0.5 g PVP-25000, and Sample D is PVP-40k-SPION synthesized at 80 °C with 0.5 g PVP-40000. The effect of PVP molecular weight on the properties of PVP-SPIONs can be further studied by characterizing these samples using various techniques, such as transmission electron microscopy (TEM), X-ray diffraction (XRD), and vibrating sample magnetometry (VSM).

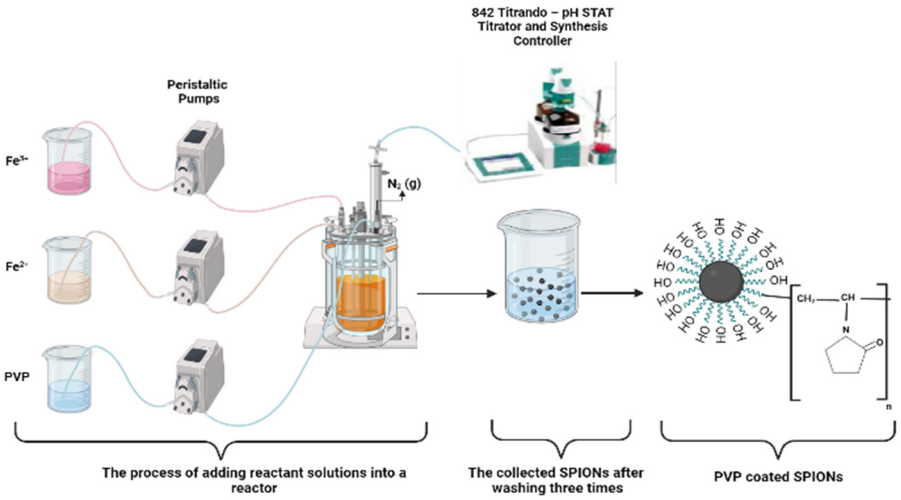

Figure 1. A schematic diagram showing the steps involved in the synthesis of bared and coated SPIONs by the co-precipitation method in a single pot.

2.3. Characterization and Instrumentation

The core size and shape of SPIONs were identified using transmission electron microscopy (TEM, Libra 120-Carl Zeiss, Munich, Germany). The phase and crystal structure of magnetic nanoparticles were analyzed by X-ray diffraction (XRD) using PANalyticalXpert PRO MRD PW 3040 diffractometers equipped with CuKα radiation source (λ = 1.5418 Å). Synthesized samples were then tested for static magnetic properties using a vibrating sample magnetometer (VSM) 8810 (10NRM). The stability and surface charge measurements of SPIONs were measured using the Malvern instrument (Nano ZS model, ZEN 3600, Worcestershire WR14 1XZ, United Kingdom).

2.4. MRI Measurements

The goal of this study was to determine the relaxivity of nanoparticle samples using a 1.5 T MRI scanner, as well as to investigate how this property varies with the size of the samples. To achieve this, five phantoms were created by mixing PVP40K-SPIONs at different concentrations (0.0625, 0.125, 0.25, 0.5, and 1 mM) into a 1% agar gel solution. Relaxometry measurements were then performed on these phantoms using both an inversion recovery sequence to measure the longitudinal relaxometry T_1 values and a spin-echo sequence to measure the transverse relaxation time T_2.

In the T_1 measurements, the echo time (TE) was fixed at 10 ms, while the repetition time (TR) values were varied (100, 150, 200, 300, 600, 1200, 2400, 4800, and 8000 ms). This allowed for the measurement of the MRI signals at different time points. Similarly, in the T_2 measurements, the repetition time (TR) was fixed at 1000 ms, and the echo time (TE) values were varied (10, 15, 20, 30, 60,120, and 200 ms).

The relaxivity values of the samples were then calculated by measuring the slope of the linear plots of reciprocal relaxation time versus Fe concentration. This data suggests that the relaxivity of the nanoparticle samples increases with increasing Fe concentration, indicating that the nanoparticles have a higher proton relaxation rate. The reason for this is that the increased Fe concentration generates a larger magnetic field, causing proton spins to relax more quickly, which generates a stronger signal. The higher relaxation rate of nanoparticles allows for more efficient imaging and diagnostics.

3. Results and Discussion

3.1. XRD Analysis

The X-ray diffraction (XRD) patterns of bare and coated superparamagnetic iron oxide nanoparticles (SPIONs) were studied, and the results are presented in Figure 2. The diffraction peaks of the samples were found at 2θ values of 30.14° (220), 35.44° (311), 43.24° (400), 53.58° (422), 57.18° (511), and 62.73° (440), respectively. The positions of XRD peaks reflected the magnetite (Fe_3O_4) phase with cubic inverse spinel structure by comparison with standard data of magnetite (JCPDS card No. 01-075-0449) [18]. A comparison of XRD patterns of coated and bare magnetite nanoparticles indicates that the peaks are similar. This suggests that the coating does not significantly alter the crystalline structure of the particles. As a result, magnetite nanoparticles were coated successfully, and their structure was preserved. The crystal structure of magnetite nanoparticles is essential for their superior magnetic properties. In this context, any alteration to its structure might lead to a reduction in its effectiveness as an MRI contrast agent. Therefore, maintaining the crystal structure of contrast agents is highly recommended when using them in MRI applications. The average crystallite size of the samples was estimated using the Scherrer equation (Equation (1)) [19], which allowed us to calculate the average crystallite size of the as-synthesized samples.

$$D_P = \frac{K\lambda}{\beta cos\theta} \quad (1)$$

where D_p is the mean crystallite size of the as-prepared samples, K is a constant related to the geometrical shape factor(0.9), λ is the X-ray wavelength (1.5406° A), β is the diffraction width at half of the maximum intensity (FWHM) in radians, and θ is the Bragg's angle at

the highest XRD peak. The average crystallite sizes of SPIONs synthesized at different concentrations of PVP were determined using X-ray diffraction analysis. The results showed that the crystallite sizes were 10.52, 10.12, 10.36, and 11.28 nm for SPIONs synthesized at 0, 10K-PVP, 25K-PVP, and 40K-PVP, respectively. Notably, the crystallite size did not change significantly with increasing PVP molecular weight, suggesting that the molecular weight of PVP does not play a significant role in the nucleation and crystal growth mechanisms of SPIONs [20]. XRD analysis of the SPIONs sample synthesized at 40K PVP, however, revealed higher crystallinity, as evidenced by the sharpness and narrowness of the main peaks compared to other samples [21]. This increase in crystallinity can be attributed to the larger crystallite size, which is inversely proportional to the width of the main peak (FWHM), as per the Scherrer formula [22]. Overall, the XRD results provide an insight into the structural characteristics of the SPIONs and suggest that PVP coating does not alter the magnetic properties of the nanoparticles while allowing us to improve their stability and biocompatibility.

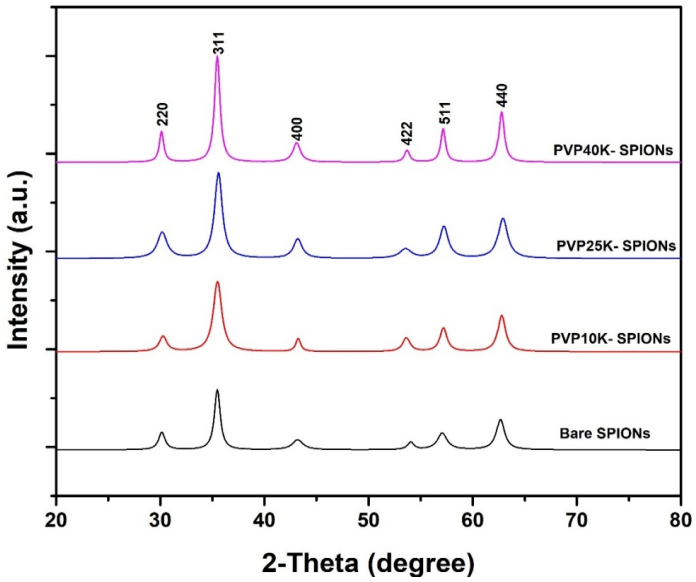

Figure 2. X-ray diffraction (XRD) patterns of bare and coated superparamagnetic iron oxide nanoparticles (SPIONs) synthesized through the one pot co-precipitation method.

3.2. TEM Results and Analysis

The morphological characteristics of superparamagnetic iron oxide nanoparticles (SPIONs) synthesized with and without polyvinylpyrrolidone (PVP) were examined using transmission electron microscopy (TEM) analysis. The TEM images and corresponding histograms of the SPIONs are presented in Figure 3. For each sample, an extensive analysis was performed on a sample of at least 200 randomly chosen nanoparticles utilizing the Image J software to determine their size distribution [23]. The results obtained from this analysis provided a comprehensive understanding of the size distribution of the nanoparticles under investigation, allowing for a deeper insight into their properties and behavior.

The TEM analysis revealed that the average particle size of bare SPIONs was found to be 10.98 nm, and they were observed to have a quasi-spherical shape. However, the TEM images of bare SPIONs also showed large agglomerates, indicating a broad size distribution. In contrast, the average particle size of SPIONs coated with PVP10K, PVP25K, and PVP40K were 9.36, 10.03, and 11.61 nm, respectively. The results from TEM measurements showed slightly larger particle diameters compared to the crystal sizes observed from XRD analysis, due to the presence of nanocrystalline surface layers. Nevertheless, both methods provided consistent results. Among the coated samples, PVP40-SPIONs exhibited more homogenous nanoparticles with a narrower size distribution and spherical shape, which is likely due to

the higher molecular weight of PVP. Furthermore, the shape of PVP40-SPIONs will appear spherical due to the lower energy effect [24]. This result reveals that the higher molecular weight of PVP plays a significant role in changing the NPs' shape, as well as limiting their agglomeration in a solvent [25].

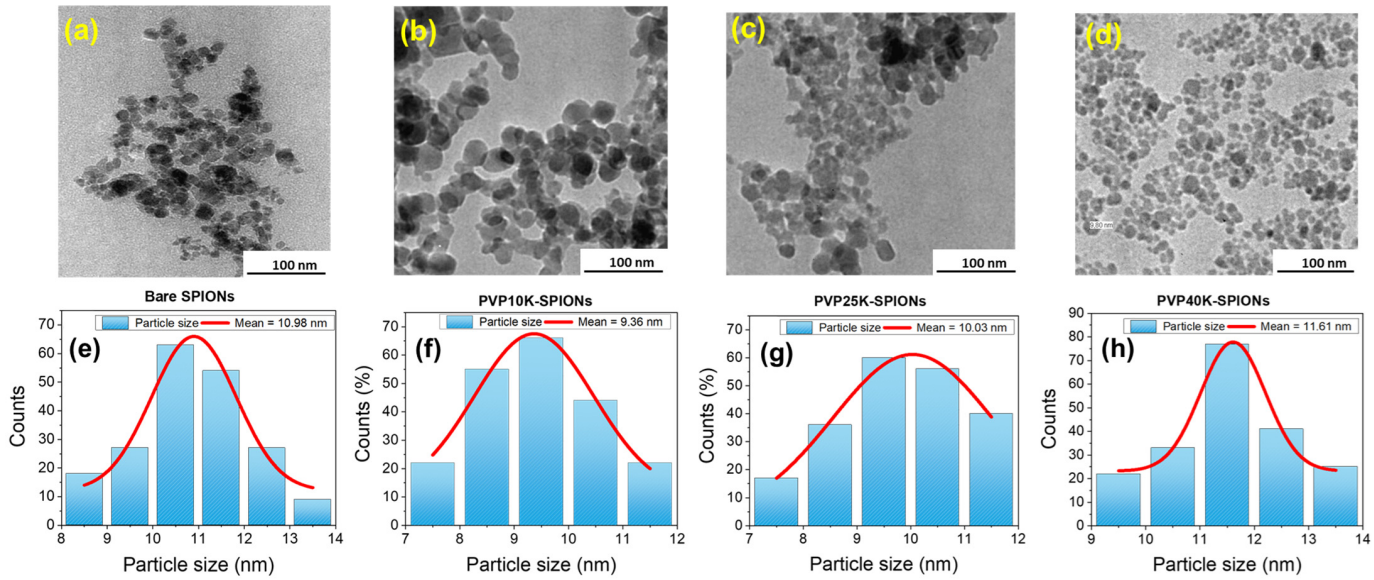

Figure 3. TEM images and size histograms analysis of bare and PVP-coated SPIONs synthesized via one-pot co-precipitation method, showing the morphological properties and size distribution of the nanoparticles. TEM images are presented in the first row (**a**–**d**): (**a**) bare SPIONs, (**b**) PVP10K-SPIONs, (**c**) PVP25K-SPIONs, and (**d**) PVP40K-SPIONs. Particle size distributions, measured in nanometers, are shown in the second row (**e**–**h**): (**e**) bare SPIONs, (**f**) PVP10K-SPIONs, (**g**) PVP25K-SPIONs, and (**h**) PVP40K-SPIONs.

The TEM result and analysis highlights the key role played by the molecular weight of PVP in shaping the nanoparticles and limiting their agglomeration in a solvent. The PVP coating effectively reduced the aggregation of nanoparticles and improved the monodispersity of the particles. Additionally, the spherical shape of PVP40-SPIONs can be beneficial for certain applications, such as biomedical imaging, as it improves the stability of the nanoparticles and allows for a more uniform distribution in biological systems. Overall, the results of this study demonstrate the potential of using PVP as a coating material to control the morphological properties of SPIONs and improve their potential applications.

3.3. Zeta Potential Measurements

The zeta potential (ζ) measurements of SPIONs samples are illustrated graphically in Figure 4. Zeta potential is a measure of the surface charge of nanoparticles, and it plays a crucial role in determining the colloidal stability of nanoparticles in solution. It is the electrostatic potential at the shear plane, which is the interface between the particle surface and the surrounding medium. Generally, nanoparticles with zeta potential values between ($\pm$40 to $\pm$60) have excellent colloidal stability in solution, whereas NPs with zeta values between $-$30 mV and +30 mV will experience rapid agglomeration and precipitation of suspension [26]. Due to their higher zeta potential values, particles with a higher repulsive force between them are able to disperse more readily in solution. This prevents them from clumping together and agglomerating. Thus, particles with zeta potential values between $\pm$40 to $\pm$60 mV will have enough repulsive forces to keep them stabilized and suspended in a solution. However, if the zeta potential is too low, the particles will aggregate and precipitate out of solution. A bare SPION has a lower zeta potential (+9.2 ev) and is unstable due to its large surface area and high energy [27]. To ensure stability, it is essential to modify the surface of SPIONs to increase their zeta potential and reduce the tendency to form

agglomerates. By increasing the zeta potential of SPIONs, the surface energy is reduced, and particle stability is improved. Furthermore, the positive charge of the zeta potential value indicates the presence of Fe ions on the surface of SPIONs [28].

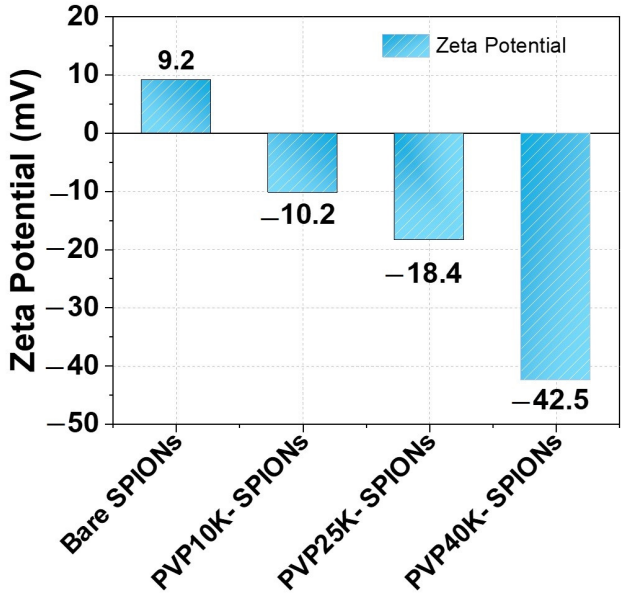

Figure 4. Graphical representation of zeta potential values for bare SPIONs and coated SPIONs.

The ζ values of PVP10k-SPIONs, PVP25k-SPIONs, and PVP40k-SPIONs are −10.2 ev, −18.4 ev, and −42.5 ev, respectively, confirming successfully binding PVP onto the surface of SPIONs, as depicted in Figure 4. The difference in ζ values of coated SPIONs can be traced to the difference in chain length of functional groups. As a consequence, more carbonyl and amino groups adsorb onto the surface of SPIONs, which contribute to the increase in steric repulsion [29]. The results show that PVP-40K-SPIONs are very stable [30]. A higher molecular weight of PVP can adsorb more ions from SPION's surface, corresponding to an increase in zeta potential. This indicates the strong electrostatic interaction between PVP and SPIONs, resulting in increased stability of the PVP-40K-SPIONs. Consequently, there is a higher electrostatic repulsion between the PVP-40K molecules, resulting in greater steric stability of the PVP-40K-SPIONs.

3.4. VSM Results and Analysis

The magnetic properties of all SPIONs samples were examined using vibrating sample magnetometry (VSM) at room temperature. The hysteresis loop, as illustrated in Figure 5, displayed a small degree of hysteresis that is considered negligible and can be safely disregarded for all samples, confirming the superparamagnetic behavior of the nanoparticles [31]. The saturation magnetization value (Ms) of bare SPIONs is 36.3 emu/g, indicating that the sample has excellent magnetic properties. According to previous studies, bare SPIONs can easily change from magnetite to maghemite during washing and preparation [32], thereby altering their magnetic properties. In Figure 5, the Ms value indicates that the coated nanoparticles have a high magnetic saturation, which implies that their magnetic properties have been preserved. As a result, coating NPs with PVP-polymer during synthesis improves saturation magnetization and allows for particle size control [33]. SPIONs coated with 10 kPVP, 25 kPVP, and 40 kPVP have Ms values of 22.2 emu/g, 24.2 emu/g, and 48.4 emu/g, respectively, which increase with the increase in the particle size of samples [34,35]. The weight measurements include the weight of the entire particles, including any PVP coating, so the magnetization values have not been adjusted for the PVP weight.

However, the higher magnetization for PVP40k-SPIONs can be attributed to decreasing the influence of the outer shell of NPs. The increased saturation magnetization can be attributed to the stabilizing effect of the polymer coating on the NPs. On the other

hand, the lower magnetization of the other coated SPIONs is due to the existence of a non-collinear magnetic outermost shell of thickness that rises comparatively with reducing particle size [36,37]. These findings reveal that PVP40k-SPIONs display excellent magnetic behavior and can be used for MRI contrast agents.

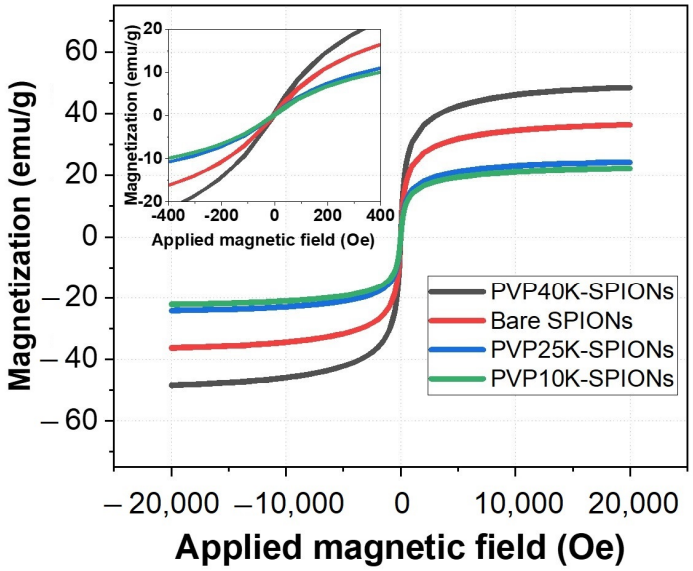

Figure 5. Magnetization curves at room temperature for bare SPIONs and SPIONs coated with different molecular weight of PVP. The inset represents the magnetic behavior of all investigated samples at low applied magnetic field.

3.5. Cytotoxicity Assay of Bare and PVP40K-SPIONs in T-Cells

The cytotoxicity of both bare and PVP40K-SPIONs was assessed using MTT assay on T-cells with five varying concentrations (0.25, 0.5, 1.0, 1.25, and 1.5 mg/mL) as final concentrations, as presented in Figure 6. Previous studies have shown that the cytotoxicity of SPIONs was observed to be higher than 1 mg/mL in vitro, depending on their surface modification, particle size, cell type, and charge [38].

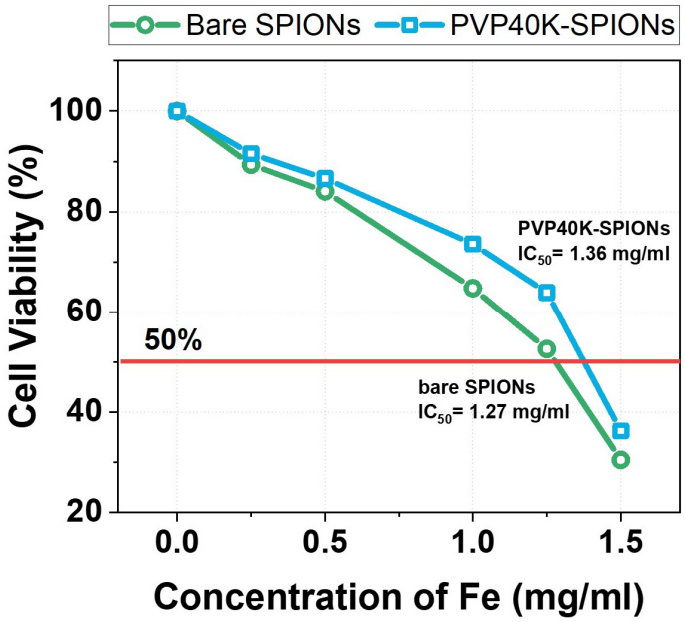

Figure 6. Cytotoxicity of bare SPIONs and PVP40K-SPIONs on T-Cells.

Figure 6 depicts a blue line that indicates the half maximal inhibitory concentration (IC50), or the concentration at which 50% cell viability is inhibited. The IC50 of PVP40K-SPIONs was found to be 1.44 mg/mL, while that of bare SPIONs was 1.38 mg/mL. At concentrations below 1.0 mg/mL, PVP40K-SPIONs did not display any cytotoxic effects on T-cells, and the cells remained over 75% viable compared to the control. The reduced cytotoxicity of PVP40K-SPIONs can be attributed to the improved biocompatibility imparted by the PVP40K coating. Our findings suggest that surface modification of SPIONs plays a critical role in determining their cytotoxicity. Based on the in vitro cytotoxicity results, it can be inferred that PVP40K-SPIONs can be used as a contrast agent for biomedical applications in MRI at concentrations below 1.0 mg/mL, with the concentration being determined as conservatively as possible.

3.6. Relaxometry Measurements of SPIONs

The use of the bare SPIONs and PVP40K-SPIONs as contrast agents in MRI was studied using 1.5 T MRI scanner. As shown in Figure 7, the longitudinal and transverse relaxivities (r_1 and r_2) of the samples were measured from the slope of the linear fit of $1/T_1$ and $1/T_2$, respectively, against Fe concentration. Values for r_1, r_2, and (r_2/r_1) ratio have been measured to determine the efficiency of the sample as a MRI contrast agent [39,40].

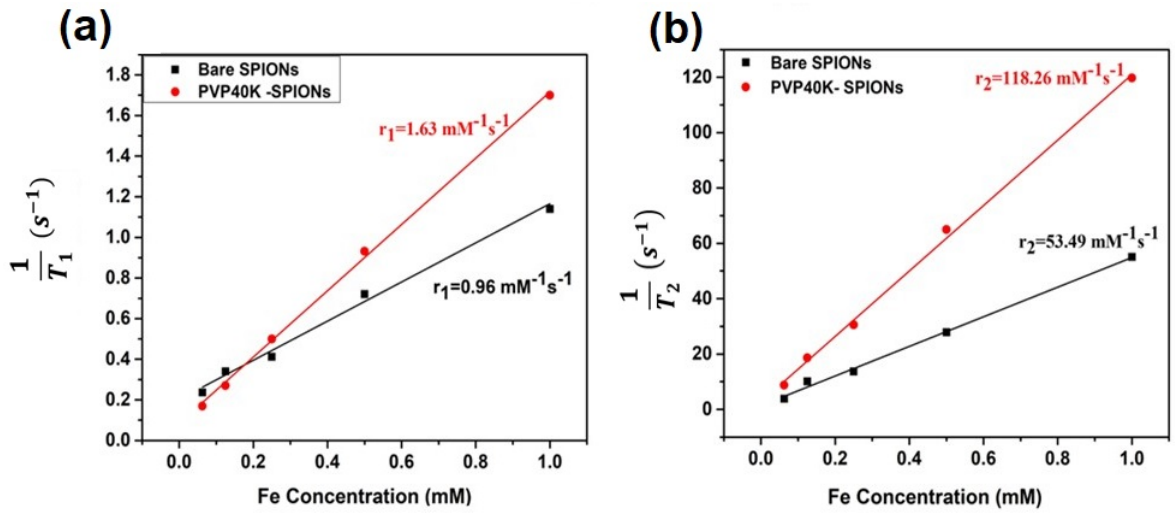

Figure 7. (**a**) Longitudinal relaxation rates ($1/T_1$), (**b**) transverse relaxation rates ($1/T_2$) of bare SPIONs and PVP40K-SPIONs with different concentrations of iron measured at 1.5 T.

The longitudinal relaxivity (r_1) of bare SPIONs and PVP40-SPIONs were found to be 0.96 and 1.63 $mM^{-1}s^{-1}$, respectively. The longitudinal relaxation time (T_1) contrast shown by our samples was not observable compared to that of the transverse relaxation time (T_2) shown on T_2 -weighted MRI image. Thus, only the T_2 contrast property of the sample was highlighted in this study. However, the transverse relaxivity (r_2) of 53.49 and 118.26 $mM^{-1}s^{-1}$ are observed respectively for bare SPIONs and PVP40K-SPIONs. The obtained results can be attributed to the higher saturation magnetization and larger particle size of PVP40-SPIONs compared to bare SPIONs [41,42]. The relaxivity ratio (r_2/r_1) is 55.72 and 72.55 for bare SPIONS and PVP40-SPIONs, respectively. This result indicates that the PVP40-SPIONs can be used as an efficient T_2-MRI contrast agent [43,44].

4. Conclusions

In summary, the effect of PVP molecular weight on the physicochemical properties of SPIONs prepared by a novel one-pot coprecipitation method was studied. Our investigations and analysis concluded that PVP-40K was the optimal choice to synthesize SPIONs with an excellent particle size distribution, as confirmed by TEM analysis. SPIONs coated with PVP-40K exhibited excellent crystallinity and enhanced magnetization,

as demonstrated by XRD and VSM analyses. Therefore, PVP-40K was selected for the synthesis of SPIONs with the narrowest particle size distribution and excellent stability. The effectiveness of the synthesized samples as contrast agents for T_2-weighted MRI was investigated. The high ratio for (r_2/r_1) PVP40K-SPIONs indicates its potential to be used as a promising contrast agent for T_2-weighted MRI. The results of our study reveal that PVP-40K coated SPIONs are a highly attractive option as contrast agents in MRI due to their exceptional biocompatibility and stability. This makes them the perfect choice for a wide range of diagnostic and MRI imaging applications.

Author Contributions: Funding acquisition F.Y.A., H.M.A.-K. and M.K.A.; Investigation O.A.N., F.Y.A., H.M.A.-K. and M.K.A.; Supervision F.Y.A., H.M.A.-K. and M.K.A.; Project administration F.Y.A., H.M.A.-K. and M.K.A.; Writing—review & editing O.A.N., F.Y.A., H.M.A.-K., M.K.A., T.A.Z., G.N.M. and A.A.; Writing—original draft O.A.N. and T.A.Z.; Methodology O.A.N., F.Y.A., H.M.A.-K. and M.K.A.; Formal analysis O.A.N., T.A.Z., G.N.M. and A.A.; Conceptualization O.A.N. and T.A.Z.; Data curation O.A.N., F.Y.A., H.M.A.-K., T.A.Z. and M.K.A.; Visualization T.A.Z. and O.A.N.; Validation O.A.N., T.A.Z. and G.N.M. All authors have read and agreed to the published version of the manuscript.

Funding: The authors thank the Deanship of Research at Jordan University of Science and Technology for supporting and funding this research project (Grant # 55/2020).

Data Availability Statement: Not applicable.

Conflicts of Interest: The authors declare no conflict of interest.

References

1. Arbab, A.S.; Wilson, L.B.; Ashari, P.; Jordan, E.K.; Lewis, B.K.; Frank, J.A. A Model of Lysosomal Metabolism of Dextran Coated Superparamagnetic Iron Oxide (SPIO) Nanoparticles: Implications for Cellular Magnetic Resonance Imaging. *NMR Biomed.* **2005**, *18*, 383–389. [CrossRef] [PubMed]
2. Shapiro, E.M.; Skrtic, S.; Sharer, K.; Hill, J.M.; Dunbar, C.E.; Koretsky, A.P. MRI Detection of Single Particles for Cellular Imaging. *Proc. Natl. Acad. Sci. USA* **2004**, *101*, 10901–10906. [CrossRef] [PubMed]
3. Zschiesche, L.; Janko, C.; Friedrich, B.; Frey, B.; Band, J.; Lyer, S.; Alexiou, C.; Unterweger, H. Biocompatibility of Dextran-Coated 30 Nm and 80 Nm Sized SPIONs towards Monocytes, Dendritic Cells and Lymphocytes. *Nanomaterials* **2023**, *13*, 14. [CrossRef]
4. Benyoucef, M.; Alzoubi, T.; Reithmaier, J.P.; Wu, M.; Trampert, A. Nanostructured Hybrid Material Based on Highly Mismatched III–V Nanocrystals Fully Embedded in Silicon. *Phys. Stat. Solidi (a)* **2014**, *211*, 817–822. [CrossRef]
5. Makhadmeh, G.N.; Abuelsamen, A.; Al-Akhras, M.-A.H.; Aziz, A.A. Silica Nanoparticles Encapsulated Cichorium Pumilum as a Promising Photosensitizer for Osteosarcoma Photodynamic Therapy: In-Vitro Study. *Photodiagn. Photodyn. Ther.* **2022**, *38*, 102801. [CrossRef]
6. Makhadmeh, G.N.; Abdul Aziz, A.; Abdul Razak, K.; Abu Noqta, O. Encapsulation Efficacy of Natural and Synthetic Photosensitizers by Silica Nanoparticles for Photodynamic Applications. *IET Nanobiotechnol.* **2015**, *9*, 381–385. [CrossRef]
7. Dheyab, M.A.; Aziz, A.A.; Jameel, M.S.; Noqta, O.A.; Khaniabadi, P.M.; Mehrdel, B. Excellent Relaxivity and X-Ray Attenuation Combo Properties of Fe_3O_4@ Au CSNPs Produced via Rapid Sonochemical Synthesis for MRI and CT Imaging. *Mater. Today Commun.* **2020**, *25*, 101368. [CrossRef]
8. Shubayev, V.I.; Pisanic, T.R.; Jin, S. Magnetic Nanoparticles for Theragnostics. *Adv. Drug Deliv. Rev.* **2009**, *61*, 467–477. [CrossRef]
9. Noqta, O.A.; Sodipo, B.K.; Aziz, A.A. One-Pot Synthesis of Highly Magnetic and Stable Citrate Coated Superparamagnetic Iron Oxide Nanoparticles by Modified Coprecipitation Method. *Funct. Compos. Struct.* **2020**, *2*, 045005. [CrossRef]
10. Noqta, O.A.; Aziz, A.A.; Usman, I.A.; Bououdina, M. Recent Advances in Iron Oxide Nanoparticles (IONPs): Synthesis and Surface Modification for Biomedical Applications. *J. Supercond. Nov. Magn.* **2019**, *32*, 779–795. [CrossRef]
11. Koczkur, K.M.; Mourdikoudis, S.; Polavarapu, L.; Skrabalak, S.E. Polyvinylpyrrolidone (PVP) in Nanoparticle Synthesis. *Dalton Trans.* **2015**, *44*, 17883–17905. [CrossRef] [PubMed]
12. Ziaei-Azad, H.; Semagina, N. Bimetallic Catalysts: Requirements for Stabilizing PVP Removal Depend on the Surface Composition. *Appl. Catal. A Gen.* **2014**, *482*, 327–335. [CrossRef]
13. Tan, X.; Wang, Z.; Yang, J.; Song, C.; Zhang, R.; Cui, Y. Polyvinylpyrrolidone-(PVP-) Coated Silver Aggregates for High Performance Surface-Enhanced Raman Scattering in Living Cells. *Nanotechnology* **2009**, *20*, 445102. [CrossRef]
14. Tang, X.-L.; Jiang, P.; Ge, G.-L.; Tsuji, M.; Xie, S.-S.; Guo, Y.-J. Poly (N-Vinyl-2-Pyrrolidone)(PVP)-Capped Dendritic Gold Nanoparticles by a One-Step Hydrothermal Route and Their High SERS Effect. *Langmuir* **2008**, *24*, 1763–1768. [CrossRef]
15. Zhang, Y.; Liu, J.-Y.; Ma, S.; Zhang, Y.-J.; Zhao, X.; Zhang, X.-D.; Zhang, Z.-D. Synthesis of PVP-Coated Ultra-Small Fe_3O_4 Nanoparticles as a MRI Contrast Agent. *J. Mater. Sci. Mater. Med.* **2010**, *21*, 1205–1210. [CrossRef]

16. Al-Fandi, M.; Oweis, R.J.; Albiss, B.A.; Alzoubi, T.; Al-Akhras, M.; Qutaish, H.; Khwailah, H.; Al-Hattami, S.; Al-Shawwa, E. A Prototype Ultraviolet Light Sensor Based on ZnO Nanoparticles/Graphene Oxide Nanocomposite Using Low Temperature Hydrothermal Method. *IOP Conf. Ser. Mater. Sci. Eng.* **2015**, *92*, 012009. [CrossRef]
17. Lee, H.Y.; Lim, N.H.; Seo, J.A.; Yuk, S.H.; Kwak, B.K.; Khang, G.; Lee, H.B.; Cho, S.H. Preparation and Magnetic Resonance Imaging Effect of Polyvinylpyrrolidone-coated Iron Oxide Nanoparticles. *J. Biomed. Mater. Res. Part B Appl. Biomater. Off. J. Soc. Biomater. Jpn. Soc. Biomater. Aust. Soc. Biomater. Korean Soc. Biomater.* **2006**, *79*, 142–150. [CrossRef]
18. Abu-Noqta, O.; Aziz, A.; Usman, A. Colloidal Stability of Iron Oxide Nanoparticles Coated with Different Capping Agents. *Mater. Today Proc.* **2019**, *17*, 1072–1077. [CrossRef]
19. Uvarov, V.; Popov, I. Metrological Characterization of X-Ray Diffraction Methods at Different Acquisition Geometries for Determination of Crystallite Size in Nano-Scale Materials. *Mater. Charact.* **2013**, *85*, 111–123. [CrossRef]
20. Li, J.; Inukai, K.; Takahashi, Y.; Tsuruta, A.; Shin, W. Effect of PVP on the Synthesis of High-Dispersion Core–Shell Barium-Titanate–Polyvinylpyrrolidone Nanoparticles. *J. Asian Ceram. Soc.* **2017**, *5*, 216–225. [CrossRef]
21. Martinez, L.; Leinen, D.; Martin, F.; Gabas, M.; Ramos-Barrado, J.; Quagliata, E.; Dalchiele, E. Electrochemical Growth of Diverse Iron Oxide (Fe_3O_4, α-FeOOH, and γ-FeOOH) Thin Films by Electrodeposition Potential Tuning. *J. Electrochem. Soc.* **2007**, *154*, D126. [CrossRef]
22. Speakman, S.A. Estimating Crystallite Size Using XRD. *MIT Cent. Mater. Sci. Eng.* **2014**, *2*, 14.
23. Lu, P.; Fang, S.; Cheng, W.; Huang, S.; Huang, M.; Cheng, H. Characterization of Titanium Dioxide and Zinc Oxide Nanoparticles in Sunscreen Powder by Comparing Different Measurement Methods. *J. Food Drug Anal.* **2018**, *26*, 1192–1200. [CrossRef]
24. Ahmed, B.; Kumar, S.; Kumar, S.; Ojha, A.K. Shape Induced (Spherical, Sheets and Rods) Optical and Magnetic Properties of CdS Nanostructures with Enhanced Photocatalytic Activity for Photodegradation of Methylene Blue Dye under Ultra-Violet Irradiation. *J. Alloy. Compd.* **2016**, *679*, 324–334. [CrossRef]
25. Seo, K.; Sinha, K.; Novitskaya, E.; Graeve, O.A. Polyvinylpyrrolidone (PVP) Effects on Iron Oxide Nanoparticle Formation. *Mater. Lett.* **2018**, *215*, 203–206. [CrossRef]
26. Riddick, T.M. *Control of Colloid Stability through Zeta Potential: With a Closing Chapter on Its Relationship to Cardiovascular Disease*; Zeta-Meter, Incorporated: Staunton, VA, USA, 1968; Volume 1.
27. Seipenbusch, M.; Rothenbacher, S.; Weber, A.; Kasper, G. Interparticle Forces in Nanoparticle Agglomerates. In Proceedings of the European Aerosol Conference, Salzburg, Austria, 9–14 September 2007.
28. Ngenefeme, F.-T.J.; Eko, N.J.; Mbom, Y.D.; Tantoh, N.D.; Rui, K.W. A One Pot Green Synthesis and Characterisation of Iron Oxide-Pectin Hybrid Nanocomposite. *Open J. Compos. Mater.* **2013**, *3*, 29725.
29. Noqta, O.A.; Aziz, A.A.; Usman, A.I. *Synthesis of PVP Coated Superparamagnetic Iron Oxide Nanoparticles with a High Saturation Magnetization*; Trans Tech Publ: Zurich, Switzerland, 2019; Volume 290, pp. 301–306.
30. Choudhari, Y.; Kulthe, S.; Inamdar, N.; Shirolikar, S.; Borde, L.; Mourya, V. Combination of Low and High Molecular Weight Chitosans for the Preparation of Nanoparticles: A Novel Approach towards Sustained Drug Delivery. *J. Nanopharm. Drug Deliv.* **2013**, *1*, 376–387. [CrossRef]
31. Dheyab, M.A.; Aziz, A.A.; Jameel, M.S.; Noqta, O.A.; Khaniabadi, P.M.; Mehrdel, B. Simple Rapid Stabilization Method through Citric Acid Modification for Magnetite Nanoparticles. *Sci. Rep.* **2020**, *10*, 10793. [CrossRef]
32. Laurent, S.; Forge, D.; Port, M.; Roch, A.; Robic, C.; Vander Elst, L.; Muller, R.N. Magnetic Iron Oxide Nanoparticles: Synthesis, Stabilization, Vectorization, Physicochemical Characterizations, and Biological Applications. *Chem. Rev.* **2008**, *108*, 2064–2110. [CrossRef]
33. Paul, K.G.; Frigo, T.B.; Groman, J.Y.; Groman, E.V. Synthesis of Ultrasmall Superparamagnetic Iron Oxides Using Reduced Polysaccharides. *Bioconjug. Chem.* **2004**, *15*, 394–401. [CrossRef]
34. Gnanaprakash, G.; Philip, J.; Jayakumar, T.; Raj, B. Effect of Digestion Time and Alkali Addition Rate on Physical Properties of Magnetite Nanoparticles. *J. Phys. Chem. B* **2007**, *111*, 7978–7986. [CrossRef]
35. Lin, C.-R.; Chu, Y.-M.; Wang, S.-C. Magnetic Properties of Magnetite Nanoparticles Prepared by Mechanochemical Reaction. *Mater. Lett.* **2006**, *60*, 447–450. [CrossRef]
36. Roy, S.; Dubenko, I.; Edorh, D.D.; Ali, N. Size Induced Variations in Structural and Magnetic Properties of Double Exchange $La_{0.8}Sr_{0.2}MnO_{3-\delta}$ Nano-Ferromagnet. *J. Appl. Phys.* **2004**, *96*, 1202–1208. [CrossRef]
37. Lopez-Quintela, M.; Hueso, L.; Rivas, J.; Rivadulla, F. Intergranular Magnetoresistance in Nanomanganites. *Nanotechnology* **2003**, *14*, 212. [CrossRef]
38. Dan, D.F.M. Scott Block Copolymer Cross-Linked Nanoassemblies Improve Particle Stability and Biocompatibility of Superparamagnetic Iron Oxide Nanoparticles | SpringerLink. Available online: https://link.springer.com/article/10.1007/s11095-012-0900-8 (accessed on 9 March 2023).
39. Tromsdorf, U.I.; Bruns, O.T.; Salmen, S.C.; Beisiegel, U.; Weller, H. A Highly Effective, Nontoxic T 1 MR Contrast Agent Based on Ultrasmall PEGylated Iron Oxide Nanoparticles. *Nano Lett.* **2009**, *9*, 4434–4440. [CrossRef]
40. Kim, B.H.; Lee, N.; Kim, H.; An, K.; Park, Y.I.; Choi, Y.; Shin, K.; Lee, Y.; Kwon, S.G.; Na, H.B. Large-Scale Synthesis of Uniform and Extremely Small-Sized Iron Oxide Nanoparticles for High-Resolution T 1 Magnetic Resonance Imaging Contrast Agents. *J. Am. Chem. Soc.* **2011**, *133*, 12624–12631. [CrossRef]
41. Gossuin, Y.; Martin, E.; Vuong, Q.L.; Delroisse, J.; Laurent, S.; Stanicki, D.; Rousseau, C. Characterization of Commercial Iron Oxide Clusters with High Transverse Relaxivity. *J. Magn. Reson. Open* **2022**, *10*, 100054. [CrossRef]

42. Jun, Y.; Seo, J.; Cheon, J. Nanoscaling Laws of Magnetic Nanoparticles and Their Applicabilities in Biomedical Sciences. *Acc. Chem. Res.* **2008**, *41*, 179–189. [CrossRef]
43. Ahmad, T.; Bae, H.; Rhee, I.; Chang, Y.; Lee, J.; Hong, S. Particle Size Dependence of Relaxivity for Silica-Coated Iron Oxide Nanoparticles. *Curr. Appl. Phys.* **2012**, *12*, 969–974. [CrossRef]
44. Al Zoubi, T.; Albiss, B.; AL-Akhras, M.-A.; Qutaish, H.; Alabed, E.; Nazrul, S. NiO-Nanofillers Embedded in Graphite/PVA-Polymer Matrix for Efficient Electromagnetic Radiation Shielding. *AIP Conf. Proc.* **2019**, *2083*, 020002. [CrossRef]